Localization of phosphorylated αB-crystallin to heart mitochondria during ischemia-reperfusion

J.-K. Jin, R. Whittaker, M. S. Glassy, S. B. Barlow, R. A. Gottlieb and C. C. Glembotski

Am J Physiol Heart Circ Physiol 294:H337-H344, 2008. First published 9 November 2007; doi:10.1152/ajpheart.00881.2007

Am J Physiol Heart Circ Physiol 294: H337–H344, 2008.
First published November 9, 2007; doi:10.1152/ajpheart.00881.2007.

Localization of phosphorylated αB-crystallin to heart mitochondria during ischemia-reperfusion

J.-K. Jin, R. Whittaker, M. S. Glassy, S. B. Barlow, R. A. Gottlieb, and C. C. Glembotski

SDSU Heart Institute and Department of Biology, San Diego State University, San Diego, California

Submitted 26 July 2007; accepted in final form 4 November 2007

Jin JK, Whittaker R, Glassy MS, Barlow SB, Gottlieb RA, Glembotski CC. Localization of phosphorylated αB-crystallin to heart mitochondria during ischemia-reperfusion. *Am J Physiol Heart Circ Physiol* 294: H337–H344, 2008. First published November 9, 2007; doi:10.1152/ajpheart.00881.2007.—The cytosolic small heat shock protein αB-crystallin (αBC) is a molecular chaperone expressed in large quantities in the heart, where it protects from stresses such as ischemia-reperfusion (I/R). Upon I/R, p38 MAP kinase activation leads to phosphorylation of αBC on Ser^{59} (P-αBC-S59), which increases its protective ability. αBC confers protection, in part, by interacting with and affecting the functions of key components in stressed cells. We investigated the hypothesis that protection from I/R damage in the heart by P-αBC-S59 can be mediated by localization to mitochondria. We found that P-αBC-S59 localized to mitochondria isolated from untreated mouse hearts and that this localization increased more than threefold when the hearts were subjected to ex vivo I/R. Mitochondrial P-αBC-S59 decreased when hearts were treated with the p38 inhibitor SB-202190. Moreover, SB-202190-treated hearts exhibited more tissue damage and less functional recovery upon reperfusion than controls. I/R activates mitochondrial permeability transition (MPT) pore opening, which increases cell damage. We found that mitochondria incubated with a recombinant mutant form of αBC that mimics P-αBC-S59 exhibited decreased calcium-induced MPT pore opening. These results indicate that mitochondria may be among the key components in stressed cells with which P-αBC-S59 interacts and that this localization may protect the myocardium, in part, by modulating MPT pore opening and, thus, reducing I/R injury.

mitochondrial permeability transition; cardioprotection

αB-CRYSTALLIN (αBC), a 175-amino acid, 22-kDa member of the small heat shock protein (sHSP) family of molecular chaperones (33), comprises 3–5% of protein in the cardiac myocytes (3, 8, 17, 24). One mechanism by which αBC may protect is via direct interaction with key components in stressed cells. In cardiac myocytes, under nonstressed conditions, αBC exhibits a diffuse cytosolic localization. However, after certain stresses, cytosolic αBC redistributes to myofilament proteins (2, 5, 6, 10, 11, 26, 32), where it may help preserve contractile protein integrity and myocardial function during potentially damaging stresses, such as ischemia-reperfusion (I/R). In support of this hypothesis are studies showing that overexpression of αBC in cultured rat cardiac myocytes (27) or in hearts of transgenic mice (31) protects from I/R damage. Moreover, the targeted disruption of αBC increases sensitivity to I/R injury in mouse hearts (28).

αBC can be phosphorylated on Ser^{19}, Ser^{45}, and Ser^{59} in response to certain stresses (15, 16). In cardiac myocytes, p38 MAP kinase-mediated activation of MAP kinase-activated protein kinase-2 (MK2) is responsible for phosphorylation of Ser^{59} (14). In cultured cardiac myocytes and isolated perfused mouse and rat hearts, simulated I/R activates p38 MAP kinase (1) and increases phosphorylation of αBC on Ser^{59} (P-αBC-S59), both of which can be blocked by dominant-negative p38 or the p38 inhibitor SB-203580 (14). Overexpression of a form of αBC that mimics phosphorylation only at Ser^{59} [αBC-S19A, -S45A, and -S59E (αBC-AAE)] protects cardiac myocytes from simulated I/R-induced cell death (27). Taken together, these findings suggest that the protective effect of αBC on cardiac myocytes is enhanced upon phosphorylation on Ser^{59}; however, the mechanism of this protection remains unknown.

Since P-αBC-S59 protects against I/R injury, which is mediated in part by signals generated by mitochondria, the present study was carried out to examine the relationship between P-αBC-S59 and mitochondria.

MATERIALS AND METHODS

Animals. Approximately 100 C3H female mice (*Mus musculus;* 8–12 wk-old) were used in this study. All procedures involving animals were performed in accordance with institutional guidelines. The animal protocol was reviewed and approved by the San Diego State University Institutional Animal Care and Use Committee.

Mitochondrial isolation from mouse hearts. Mouse hearts were first fractionated into cytosolic, mitochondrial, nuclear, endoplasmic reticular, and myofibrillar fractions by differential centrifugation, essentially as previously described (26). Briefly, mouse heart ventricles were frozen in liquid nitrogen, pulverized, and then homogenized in isolation buffer (70 mM sucrose, 190 mM mannitol, 20 mM HEPES, 0.2 mM EDTA, 1 μM Na_3OV_4, 10 μg/ml aprotinin, 10 μg/μl leupeptin, 0.5 mM *p*-nitrophenylphosphate, and 1 mM phenylmethylsulfonyl fluoride). The homogenate was centrifuged at 600 *g* for 10 min, yielding a pellet consisting of nuclei and myofibrils and a supernatant containing mitochondria, endoplasmic reticulum, and cytosol. The pellet was washed twice in isolation buffer, resuspended in nuclear extraction buffer [20 mM HEPES (pH 7.9), 25% glycerol, 420 mM NaCl, 1.5 mM $MgCl_2$, and 0.2 mM EDTA], and centrifuged at 600 *g* for 10 min. The pellet contained myofibrils; because the supernatant, consisting of nuclear components, did not contain any detectable αBC, it was not analyzed further in this study. The 600-*g* supernatant was centrifuged at 5,000 *g* for 15 min; the pellet consisted of crude mitochondria. The 5,000-*g* supernatant was centrifuged at 100,000 *g* for 10 min to yield a pellet that included the rough endoplasmic reticulum. The 100,000-*g* supernatant was the cytosolic fraction. The crude mitochondria were purified further on an iodixanol density gradient (catalog no. 1114542 OptiPrep, Axis-Shield, Oslo, Norway), essentially as previously described (29). Crude mitochondria were applied to the top of the gradient and centrifuged at 100,000 *g* for 1 h at 4°C. Twenty 1-ml fractions were collected; immunoblot-

Address for reprint requests and other correspondence: C. C. Glembotski, SDSU Heart Institute and Dept. of Biology, San Diego State Univ., San Diego, CA 92182 (e-mail: cglembotski@sciences.sdsu.edu).

The costs of publication of this article were defrayed in part by the payment of page charges. The article must therefore be hereby marked "*advertisement*" in accordance with 18 U.S.C. Section 1734 solely to indicate this fact.

ting and electron microscopy showed that purified mitochondria were present in gradient *fractions 11–15*.

Transmission electron microscopy of mouse heart mitochondria. Crude and purified mitochondria were fixed with phosphate-buffered, half-strength Karnovsky's fixative, overnight at 4°C (22). After several buffer washes, the pellets were postfixed in 2% osmium tetroxide and 3% potassium ferrocyanide for 2 h on ice, rinsed in water, dehydrated through ascending concentrations of ethanol followed by 100% acetone, and then infiltrated and embedded in Eponate 12 (Ted Pella). Sections were stained with uranyl acetate and lead citrate.

Ex vivo mouse heart I/R. Ex vivo global I/R of mouse hearts was performed as previously described (28). Briefly, mice were injected with heparin (500 U/kg ip) for 10 min and then anesthetized with pentobarbital sodium (150 mg/kg). Hearts were isolated and rinsed with ice-cold modified Krebs-Henseleit buffer, the aortas were cannulated, and the hearts were mounted onto a Langendorff perfused heart apparatus. Hearts were perfused by gravity at a constant pressure of 80 mmHg, and a pressure sensor balloon was inserted into the left ventricle through the left atrium. Left ventricular developed pressure (LVDP, mmHg) was assessed using Powerlab software. Hearts were equilibrated for 30 min submersed in buffer at 37°C and paced at ~400 Hz and 0.5 mA. Hearts were subjected to global no-flow ischemia without pacing for 25 min and then reperfused for 10–30 min. In some experiments, hearts were treated with SB-202190 (catalog no. 152121-30-7, Sigma-Aldrich, St. Louis, MO), which was dissolved in DMSO and added to Krebs-Henseleit buffer. Perfusate was examined for lactate dehydrogenase (LDH) enzyme activity as previously described (26).

Preparation of recombinant αBC. The preparation of cDNAs encoding wild-type αBC (αBC-WT) or mutant αBC has been previously described (27). cDNAs encoding rat αBC and αBC-S19A, -S45A, and -S59E (i.e., αBC-AAE) were subcloned from pcDNA3.1 into pRSET-A (catalog no. V351-20, Invitrogen, Carlsbad, CA) to prepare constructs that would encode αBC-WT or αBC-AAE with an NH_2-terminal 6× His tag. These constructs were transfected into BL21 cells and then purified under native conditions on Ni-NTA Superflow columns (catalog no. 30622, Qiagen, Valencia, CA) according to the manufacturer's protocol.

Immunoblotting. Unless otherwise stated, 2–100 μg of protein were fractionated by SDS-PAGE, transferred to polyvinylidene difluoride paper, and analyzed by immunoblotting using standard techniques. Anti-αBC (catalog no. SPA-223), anti-phosphorylated (Ser^{59}) αBC (catalog no. SPA-227), and anti-glucose-regulated protein 78 (GRP-78; catalog no. SPA-826) were purchased from Stressgen; anti-MAPKAPK-2 (catalog no. 3042) and anti-phosphorylated MAPKAPK-2 (catalog no. 3044) from Cell Signaling (Danvers, MA); anti-dynamin II (catalog no. 610263) from BD Bioscience (San Jose, CA); anti-cytochrome *c* oxidase IV (catalog no. A21348) from Invitrogen; anti-lysosomal membrane protein (LAMP1; catalog no. sc-17768) from Santa Cruz Biotechnology (Santa Cruz, CA); and anti-α-actinin (catalog no. A7811) and anti-α-sarcomeric actin (catalog no. A2172) from Sigma-Aldrich.

Mitochondrial swelling assays. Mitochondrial swelling assays used to examine permeability transition pore opening were performed as previously described (35). Briefly, aliquots containing 25 μg each of mitochondrial protein were mixed with 1 nmol of recombinant protein in a 96-well plate with swelling buffer [10 mM Tris (pH 7.4), 120 mM KCl, 20 mM MOPS, and 5 mM KH_2PO_4] to 100 μl total volume and then incubated for 15 min at room temperature. Mitochondrial swelling was initiated by addition of 250 μM $CaCl_2$, and absorbance was measured for 1 h on a plate reader at 520 nm. To confirm that absorbance decreases were due to permeability transition pore opening, cyclosporin A (CsA) was added to final concentration of 15 nM.

Assessment of mitochondrial membrane potential in cultured cardiac myocytes. The effects of overexpressing various forms of αBC on mitochondrial membrane potential ($\Delta\Psi_m$) were assessed in rat primary neonatal ventricular myocytes using tetramethylrhodamine methyl ester (TMRM). Cells were infected with recombinant adenoviral (AdV) strains expressing green fluorescent protein (GFP) alone (control), GFP and rat αBC-WT, or GFP and rat αBC-AAE, each at a multiplicity of infection of 10. In these AdV strains, GFP and αBC are driven by separate cytomegalovirus promoters. The myocyte isolation and the preparation and use of these AdV strains have been described previously (27). The cells were pretreated with 20 nM TMRM for 15 min, treated with 100 μM H_2O_2 for 150 min to induce mitochondrial permeability transition (MPT) pore opening, and then viewed by fluorescence microscopy. The number of TMRM-positive cells was determined in three different fields per culture, totaling ≥200 cells per culture ($n = 3$ cultures per treatment). Results are reported as the ratio of TMRM-positive cells to the total number of cells in each field.

Statistical analyses. Unless otherwise stated, values are means ± SE. Significant differences between groups were assessed using a one-way ANOVA followed by Bonferroni's test or Newman-Keuls post hoc analysis at $P < 0.05$ or 0.01.

RESULTS

Initial studies were carried out to determine the levels of αBC in subcellular fractions prepared from mouse hearts subjected to ex vivo I/R. αBC was abundant in the cytosolic fractions prepared from control mouse hearts, as expected; however, it was nearly undetectable in cytosolic fractions prepared from hearts subjected to 25 min of ischemia followed by 10 min of reperfusion (Fig. 1, *A* and *D*), consistent with a possible redistribution of αBC to other subcellular locations. Since αBC has been reported to localize to myofibrils in rat hearts subjected to I/R (11), we examined the myofibril fractions. αBC was very low in the myofibril fractions prepared from control mouse hearts but increased by ~3.5-fold after I/R, as expected (Fig. 1, *B* and *D*), demonstrating that the myofilament fraction is one of the targets for I/R-mediated αBC redistribution. Since mitochondria are susceptible to I/R damage and mitochondrial proteins are susceptible to unfolding during I/R (13), mitochondrial fractions were examined for αBC. Some αBC was associated with mitochondria isolated from control mouse hearts; however, upon I/R, the level of mitochondrial αBC increased substantially (Fig. 1, *C* and *D*), suggesting that mitochondria are a target for αBC binding during I/R. Since I/R activates p38 and αBC phosphorylation on Ser^{59}, the levels of P-αBC-S59 were examined by immunoblotting with an antibody that cross-reacts with only this form of αBC. Under control conditions, the level of P-αBC-S59 associated with mitochondria was very low; however, after I/R, mitochondrial P-αBC-S59 increased ~3.5-fold (Fig. 1, *C* and *D*).

To confirm the localization of αBC to mitochondria, mitochondria were purified further by density gradient sedimentation. Transmission electron microscopy of samples from the differential and density gradient centrifugation steps demonstrated that the mitochondria from untreated mouse hearts were highly enriched after density gradient centrifugation (Fig. 2, *A* and *B*). Essentially all the objects in the micrograph of the gradient-purified mitochondria were intact mitochondria or clearly recognizable as mitochondrial remnants, thus supporting the high degree of purity of these mitochondria. The density gradient fractions were analyzed for αBC, as well as several marker proteins for mitochondria and potentially contaminating organelles, by immunoblotting. αBC immunoreactivity was high in the homogenate as well as in the crude mitochondrial sample (Fig. 2*C*).

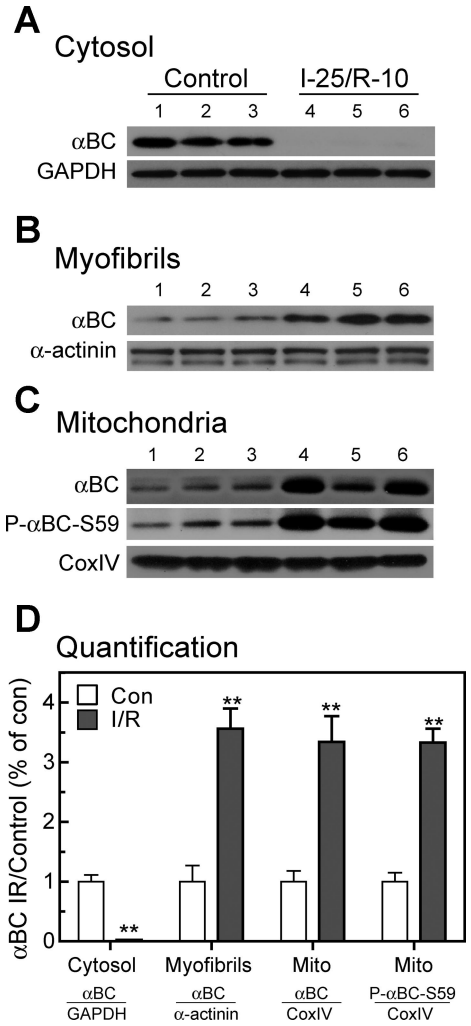

Fig. 1. Distribution of αB-crystallin (αBC) in subcellular fractions prepared from mouse hearts subjected to ex vivo ischemia-reperfusion (I/R). Mouse hearts were subjected to continual perfusion for 65 min (control) or equilibration for 30 min followed by 25 min of global ischemia and 10 min of reperfusion (I/R; $n = 3$ hearts per treatment). After perfusion, ventricular homogenates were subjected to differential centrifugation to isolate cytosol (*A*), myofibrils (*B*), and mitochondria (*C*). Portions of each fraction from each heart were then analyzed by SDS-PAGE and immunoblotting for αBC, GAPDH, α-actinin, αBC phosphorylated on Ser^{59} (P-αBC-S59), and cytochrome oxidase IV (Cox IV). *D*: αBC bands in immunoblots in *A–C* were quantified by densitometry and normalized to GAPDH, α-actinin, or cytochrome oxidase IV, which were used as loading controls for fold, myofibril, and mitochondrial fractions, respectively. Normalized values for αBC in I/R samples are plotted as fold of each control ($n = 3$ hearts per treatment). $^{**}P <$ 0.01 vs. control.

Moreover, αBC immunoreactivity in the density gradient fractions closely mirrored that of the mitochondrial specific cytochrome component cytochrome oxidase IV (Fig. 2*C*). Dynamin II, GRP-78, LAMP1, and α-actinin, which are markers for plasma membrane, rough endoplasmic reticulum, lysosomes, and myofilaments, respectively, did not comigrate with αBC and cytochrome oxidase IV. Taken together, the results in Fig. 2 demonstrate the high purity of the mouse heart mitochondria, as well as the localization of αBC to the same fraction as the purified mitochondria. Moreover, the continued association of αBC with mitochondria after migration into a density gradient further supports the relatively strong association of αBC with mitochondria.

The levels of αBC, P-αBC-S45, and P-αBC-S59 were examined in density gradient-purified mitochondria from mouse hearts subjected to ischemia or I/R. There was no significant change in the level of P-αBC-45 under any of the conditions (Fig. 3*A*). There was a small, approximately twofold, increase in αBC and P-αBC-S59 after 25 min of ischemia (Fig. 3, *A* and *B*). Mitochondrial αBC and P-αBC-S59 increased further, ~3.5-fold, when a 25-min period of ischemia was followed by 10 or 30 min of reperfusion (Fig. 3, *A* and *B*). No significant change in cytochrome oxidase IV was observed after the various treatments. These results demonstrate that the levels of mitochondrial αBC and αBC-59P increased coordinately during ischemia and I/R but that the greatest levels of mitochondrial αBC were observed after I/R. Accordingly, further experiments focused on the levels of total αBC and P-αBC-S59 with 25 min of ischemia followed by 10 min of reperfusion.

To examine the relationship between p38 activation and the levels of mitochondrial P-αBC-S59, mouse hearts were pretreated with vehicle only or with the p38 MAP kinase inhibitor SB-202190 and then subjected to ex vivo I/R. MK2, which lies directly downstream of p38 (1), was examined to ensure the efficacy of p38 inhibition by SB-202190. Immunoblots showed that I/R increased the phosphorylated, active form of MK2 in

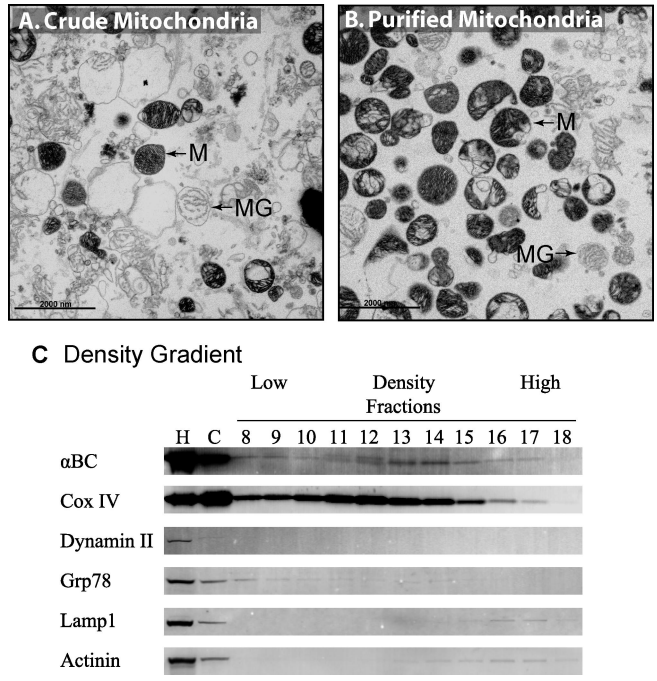

Fig. 2. Transmission electron micrographs of mouse heart mitochondria. Subsarcolemmal mitochondria were isolated by differential centrifugation (*A*) followed by iodixanol gradient centrifugation (*B*). Sedimented material from each purification step was sectioned, stained with uranyl acetate and lead citrate, and then viewed by transmission electron microscopy. Magnification ×21,000; scale bars, 2,000 nm. M, mitochondria exhibiting cristae structure; MG, mitochondrial ghosts, which appear to be mitochondria that have swelled and lost their contents. *C*: samples from iodixanol gradient analyzed by SDS-PAGE followed by immunoblotting for αBC, cytochrome oxidase IV, dynamin II, glucose-regulated protein-78 (GRP-78), lysosomal membrane protein (LAMP1), and actinin. H, homogenate; C, crude mitochondria. Low and high represent low- and high-density regions of the gradient.

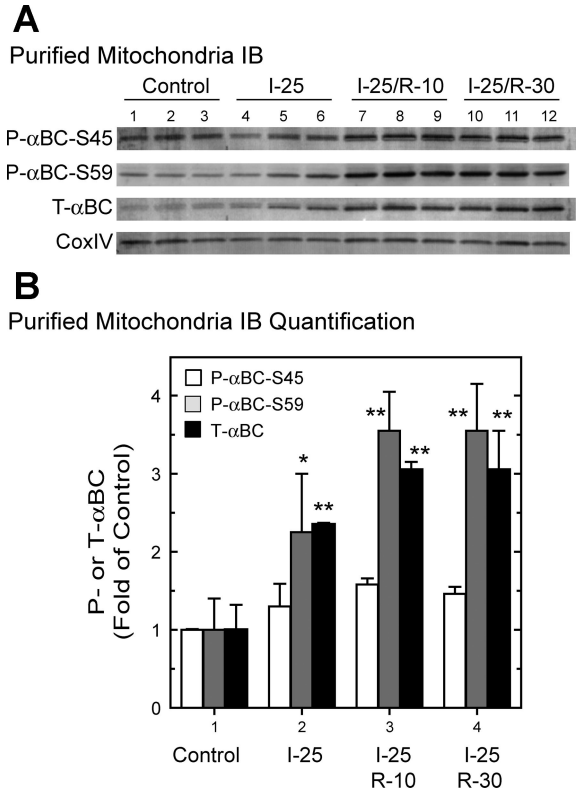

Fig. 3. Effect of ischemia or I/R on mouse heart mitochondrial αBC. *A*: perfused mouse hearts were subjected to 30 min of equilibration, during which optimal heart function on the perfusion apparatus was established. Hearts were then subjected to continued perfusion for an additional 55 min (control), global ischemia for 25 min (I-25), or global ischemia for 25 min followed by reperfusion (R) for 10 or 30 min (I-25/R-10 or I-25/R-30, $n = 3$ hearts per treatment). After each treatment, hearts were collected, and density gradient-purified mitochondria were subjected to SDS-PAGE followed by immunoblotting (IB) with antisera specific for total αBC (T-αBC), P-αBC-S45, P-αBC-59S, or cytochrome oxidase IV. *B*: quantification of immunoblots in *A*. Phosphorylated and total αBC were normalized to cytochrome oxidase IV ($n = 3$ hearts per treatment). *$P < 0.05$; **$P < 0.01$ vs. control.

an SB-202190-sensitive manner, whereas total MK2 levels were unaffected (Fig. 4, *A* and *B*), demonstrating the effective inhibition of p38 by SB-202190. SB-202190 also decreased the levels of mitochondrial P-αBC-S59 during I/R but had no effect on total mitochondrial αBC[1] (Fig. 4, *A* and *C*). These results indicate that a portion of the αBC associated with mitochondria during I/R was P-αBC-S59 and that this association can be inhibited by SB-202190.

The effects of SB-202190 on the function of hearts subjected to I/R were examined. As expected, mouse hearts that were continually perfused, and not subjected to I/R, retained relatively high LVDP, which was established as 100% (Fig. 5*A*). Moreover, perfusion with SB-202190 had no effect on LVDP in the absence of I/R (Fig. 5*A*). Hearts subjected to global ischemia exhibited a complete loss of LVDP during ischemia and a partial recovery of function on reperfusion, amounting to ~24% of maximal LVDP after 10 min of reperfusion (Fig. 5*A*). In contrast, hearts that were pretreated with SB-202190 during the equilibration period and during ischemia and I/R exhibited significantly lower recovery than the other treatment groups, amounting to ~12% of maximal LVDP after 10 min of reperfusion (Fig. 5*A*). Release of LDH was measured to esti-

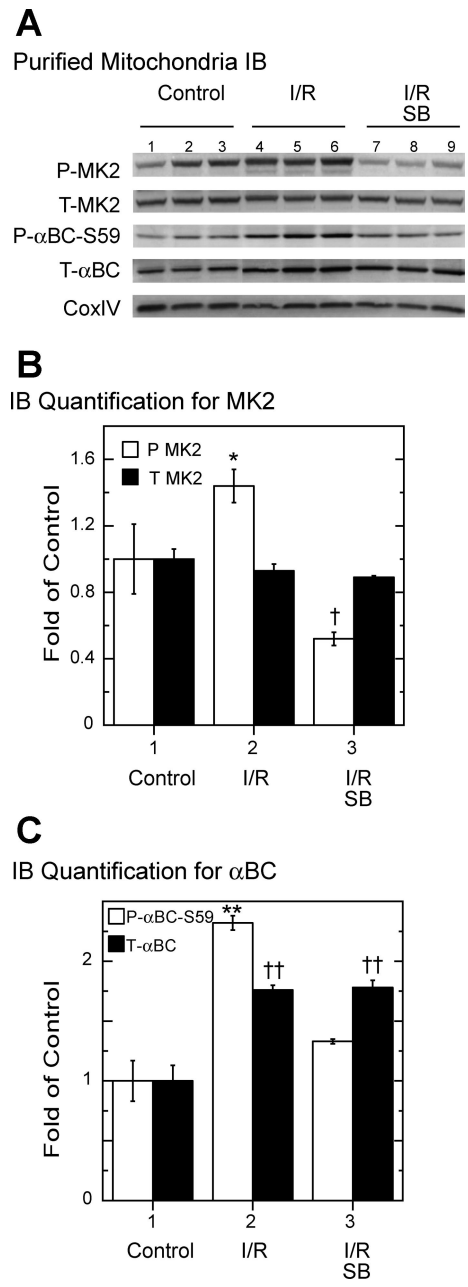

Fig. 4. Effect of SB-202190 on I/R-mediated activation of MAP kinase-activated protein kinase-2 (MK2) and on mouse heart mitochondrial αBC. *A*: hearts were subjected to 30 min of equilibration followed by continual perfusion for 35 min (control) or 25 min of global ischemia followed by 10 min of reperfusion (I/R), as described in Fig. 2 legend. In some cases, hearts were perfused during 30 min of preequilibration and 10 min of reperfusion with 10 μM SB-202190 (SB; I/R SB). After these treatments, mitochondria were purified by density gradient centrifugation and subjected to SDS-PAGE followed by immunoblotting with antisera specific for phosphorylated or total MAPKAP-K2, total αBC, P-αBC-S59, or cytochrome oxidase IV. *B*: quantification of phosphorylated and total MK2 immunoblots in *A* ($n = 3$ hearts per treatment). * or †$P < 0.05$ vs. all other values. *C*: quantification of phosphorylated and total αBC immunoblots in *A* ($n = 3$ hearts per treatment). ** or ††$P < 0.01$ vs. all other values.

[1] Depending on the experiment, we found that the increase in the total αBC associated with mitochondria upon I/R varied from ~1.5- to 3-fold.

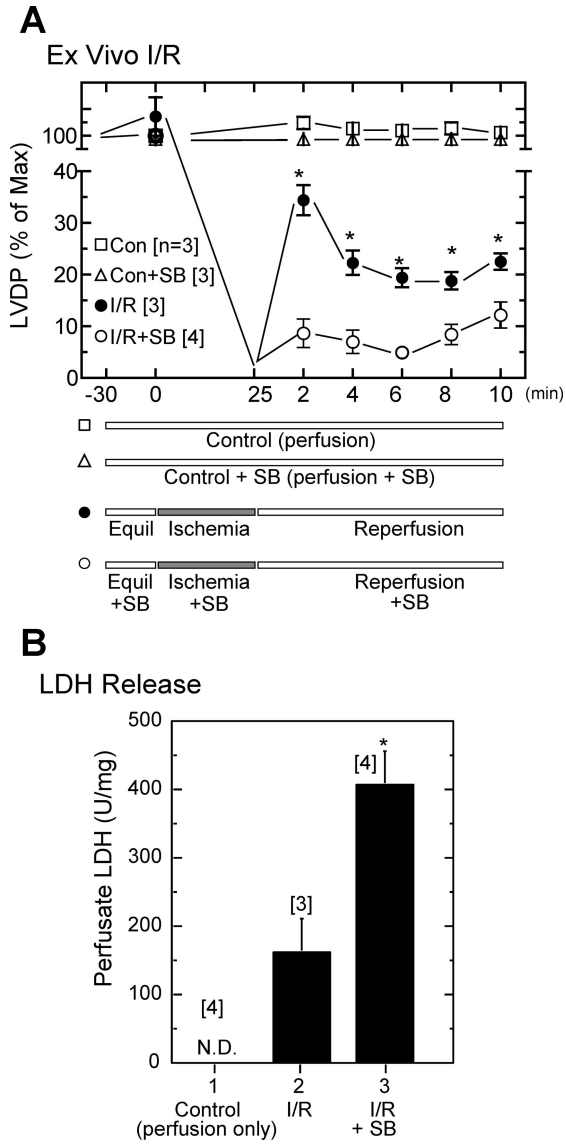

Fig. 5. Effect of SB-202190 on heart function and lactate dehydrogenase (LDH) release during I/R. *A*: mouse hearts were subjected to 30 min of equilibration with or without SB-202190 and continual perfusion for 35 min (control and control + SB) or 25 min of global ischemia followed by 10 min of reperfusion with or without 10 μM SB-202190 (I/R and I/R + SB). Left ventricles were filled with a balloon connected to a Millar pressure transducer, which enabled an estimation of relative left ventricular developed pressure (LVDP). Maximum LVDP of each heart after 30 min of preequilibration was set to 100%, and all subsequent LVDP values were normalized to that value. Values are means ± SE of numbers of hearts shown in brackets. $*P < 0.05$ vs. all other values at this time point. *B*: LDH activity in perfusate at conclusion of each experiment. Values are means ± SE of number of hearts shown in brackets. ND, not detectable. $*P < 0.05$ vs. I/R.

mate necrosis,[2] the major source of tissue damage after 10 min of reperfusion of ex vivo mouse hearts. In control, continuously perfused hearts, LDH in the perfusate was not detectable (Fig. 5*B*). However, after I/R, perfusate LDH levels reached ~150 U/mg of protein in untreated hearts and ~400 U/mg in the SB-202190-treated hearts (Fig. 5*B*). Taken together, the results in Figs. 4 and 5 indicate that pretreatment of isolated perfused mouse hearts with SB-202190 effectively inhibited p38 and MK2, reduced the quantity of mitochondrial P-αBC-S59, impaired functional recovery during reperfusion, and increased necrosis. Although SB-202190 may have widespread effects on many p38-dependent pathways, these findings are consistent with a possible role for P-αBC-S59 in affecting mitochondrial function during I/R.

I/R activates MPT pore opening, which can contribute to necrosis early in I/R and apoptosis with longer periods of I/R (12). Accordingly, swelling assays were performed with isolated mitochondria to examine the effects of P-αBC-S59 on calcium-activated MPT pore opening in vitro. In this assay, swelling is evident as a decrease in absorbance, and the extent of swelling correlates with MPT opening. In the absence of added calcium, isolated mouse heart mitochondria exhibited little swelling, as shown by moderate decreases in absorbance (Fig. 6*A*). However, upon addition of calcium, absorbance decreased rapidly, indicating increased swelling and, thus, increased MPT pore opening (Fig. 6*A*), which was significantly different from the outcome in the absence of calcium (Fig. 6*B*). CsA, an inhibitor of MPT pore opening, significantly inhibited the calcium-induced swelling (Fig. 6, *A* and *B*), confirming that some of the swelling that occurred in the absence of calcium was due to MPT pore opening but that the increased swelling observed on addition of calcium induced additional pore opening. Addition of recombinant wild-type αBC decreased mitochondrial swelling (Fig. 6*A*), but the decrease did not reach statistical significance (Fig. 6*B*). In contrast, addition of recombinant αBC-AAE, which mimics phosphorylation on Ser^{59}, resulted in a significant reduction in mitochondrial swelling, equivalent to values obtained in the absence of calcium (Fig. 6, *A* and *B*). Addition of CsA along with αBC-WT or αBC-AAE marginally decreased swelling, but these values were not statistically significantly different from those observed in the absence of calcium (Fig. 6, *A* and *B*). These findings are consistent with a possible role for mitochondrial P-αBC-S59 as an inhibitor of MPT pore opening.

To verify the results of the swelling assays, the effects of overexpression of hemagglutinin (HA)-tagged αBC-WT or HA-αBC-AAE on H_2O_2-induced MPT pore opening in cultured neonatal rat ventricular myocytes were assessed by examination of $\Delta\Psi_m$. Initial experiments demonstrated that the relative expression levels of HA-αBC-WT and HA-αBC-AAE were the same in cultures infected with AdVs encoding these forms of αBC (Fig. 7*A*). The number of TMRM-positive cells decreased by ~50% when myocytes infected with control AdV were treated with H_2O_2 (Fig. 7, *B, B′, C, C′*, and *H*), consistent with the expected loss of $\Delta\Psi_m$ as a result of H_2O_2-induced MPT pore opening. Although the number of TMRM-positive cells also decreased in response to H_2O_2 in myocytes infected with AdV-HA-αBC-WT (Fig. 7, *D, D′, E,* and *E′*), the decrease amounted to only ~20% (Fig. 7*H*), consistent with the possibility that overexpression of αBC-WT moderates the loss of $\Delta\Psi_m$ that is due to MPT pore opening. Finally, the number of TMRM-positive cells showed no significant change in response to H_2O_2 in myocytes infected with AdV-HA-αBC-AAE (Fig. 7, *D, D′, E, E′*, and *H*). Taken together, the results in Fig. 7 are consistent with the swelling assay results in Fig. 6, further supporting the hypothesis that phosphorylation on Ser^{59} enhances the ability of αBC to moderate MPT pore opening.

[2] Although widely accepted as a measure of necrosis, LDH release could also be the result of anaerobic metabolism or nonnecrotic tissue damage.

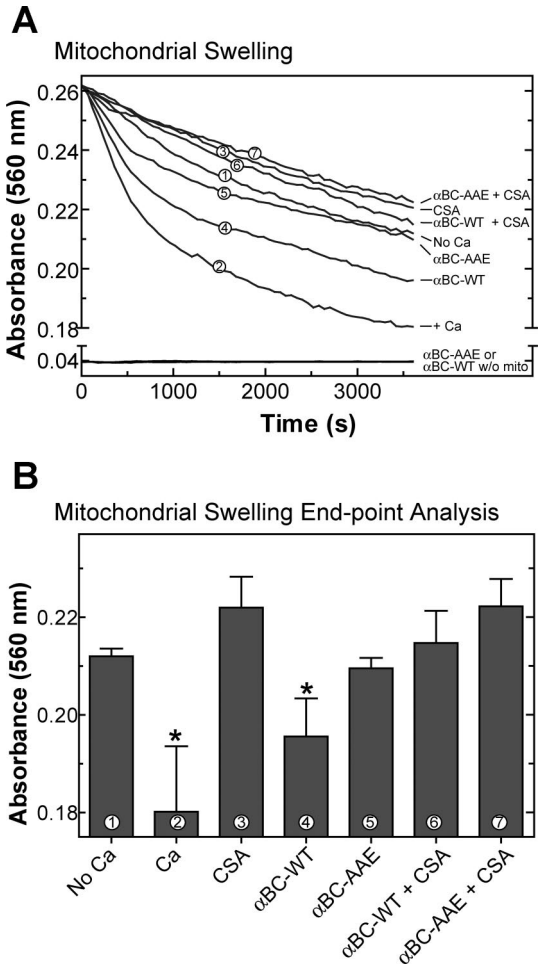

Fig. 6. Effect of αBC on calcium-induced swelling of isolated mitochondria. *A*: swelling assays were performed on mouse heart mitochondria. Decreases in absorbance in the absence of added calcium (No Ca) represent baseline swelling; absorbance changes in the presence of 250 μM calcium only (+Ca) represent maximal swelling. Addition of calcium + cyclosporin A (CsA) demonstrated that swelling was due to mitochondrial permeability transition (MPT) pore opening. Effects of addition of 1 nmol of recombinant wild-type αBC (αBC-WT) or recombinant αBC-AAE with and without CsA on calcium-induced swelling are also shown. Swelling was initiated by addition of 250 μM calcium ± various other additions. As a control for possible aggregation of recombinant αBC during the assay, effects of αBC-WT or αBC-AAE in the absence of mitochondria were examined (αBC-AAE or αBC-WT w/o mito). Absorbance at 560 nm was followed throughout the assay. Averages of compiled data are shown, but SE, which averaged ~5%, are omitted for clarity ($n = 3$ different experiments on different mitochondrial preparations). *B*: absorbance at 560 nm from *A* at the end of each experiment, i.e., at 60 min (3,600 s). Values are means ± SE. *$P < 0.05$, αBC-WT vs. Ca.

DISCUSSION

Previous studies have shown that αBC protects the heart from I/R damage (28, 31). During I/R, p38-mediated activation of MK2 results in phosphorylation of αBC on Ser[59] (14–16), generating a form of αBC that protects cultured cardiac myocytes from simulated I/R-induced cell death (27). The results of the present study extend these earlier findings, showing that I/R increases mitochondrial αBC, a portion of which is P-αBC-S59. Moreover, the present study showed that inhibiting the mitochondrial localization of only P-αBC-S59 did not affect the mitochondrial levels of other forms of αBC but decreased functional recovery upon I/R, supporting the possibility that the effect of P-αBC-S59 on the heart is different from the effect of other forms of αBC. Finally, a form of αBC that mimics P-αBC-S59, αBC-AAE, effectively inhibited MPT pore opening on mitochondria, in vitro, consistent with a functional role for this form of αBC at the mitochondrial level. The latter findings are consistent with two recent studies showing an increase in calcium-induced MPT pore opening in mitochondria prepared from mice that lack αBC compared with wild-type mouse mitochondria (18, 36).

What function(s) might αBC exert upon association with mitochondria? Since αBC is a molecular chaperone, it is probable that it exerts its protective effects by binding to other proteins on or in mitochondria. For example, P-αBC-S59 may bind to and modulate the function of MPT pore proteins. Such an effect could account for our observation that αBC-AAE decreases calcium-inducible mitochondrial swelling in vitro. In further support of this possibility is a recent finding that mutations that mimic αBC phosphorylation increase its chaperone function (9). αBC could also localize to mitochondria as a member of signaling complexes that translocate to mitochondria upon I/R stress. In support of this possibility is the finding that p38 and MK2, both of which can form a complex with αBC, translocate to mitochondria during certain stresses (30). Also, HSP27, which can also reside in a complex with p38 and MK2, has been found to associate with mitochondria (37).

What is the stimulus for αBC movement to mitochondria? αBC may localize to stressed mitochondria in response to unfolding of mitochondrial proteins. For example, the outer mitochondrial membrane protein TOM20, a member of a mitochondrial protein translocase, is prone to unfolding on myocardial ischemic stress, and by maintaining TOM20 structure, other HSPs, e.g., HSP70, contribute to the protective effects of ischemic preconditioning (4). Additionally, the unfolding of MPT pore proteins during oxidative stress might attract αBC to the mitochondrial surface. Consistent with this possibility are studies showing that one mechanism by which MPT is activated is the unfolding of MPT pore proteins upon stress (13). In addition to binding to the surface of mitochondria, recent electron-micrographic studies provide evidence that αBC can localize to the inside of mitochondria (36). Such conditional localization of cytosolic sHSPs to the interior of mitochondria has also been shown for HSP25, which binds to and protects cytochrome complex I from oxidative stress in PC12 cell mitochondria (7). The possibility that sHSP, similar to αBC and HSP25, can gain entry into mitochondria is intriguing, since they do not possess known mitochondrial translocation sequences, and further studies are required to determine the responsible mechanism.

In addition to binding to mitochondria, αBC interacts with other structures in cardiac myocytes, such as myofilaments, where it might provide stability against stress-induced unfolding. Moreover, in other cell types, αBC interacts with cytosolic proteins to provide protection. For example, in cultured breast carcinoma cells, αBC binds to pro-caspase-3 and inhibits the autoproteolytic generation of caspase-3 (19, 20). αBC also binds to and inhibits tumor necrosis factor apoptosis-inducing ligand (TRAIL) in breast carcinoma cells and, in so doing, exerts an antiapoptotic effect by blocking TRAIL-mediated caspase-3 activation (21). αBC has also been shown to bind to p53, which inhibits its translocation to mitochondria, thus modulating peroxide-mediated apoptosis in mouse C2C12

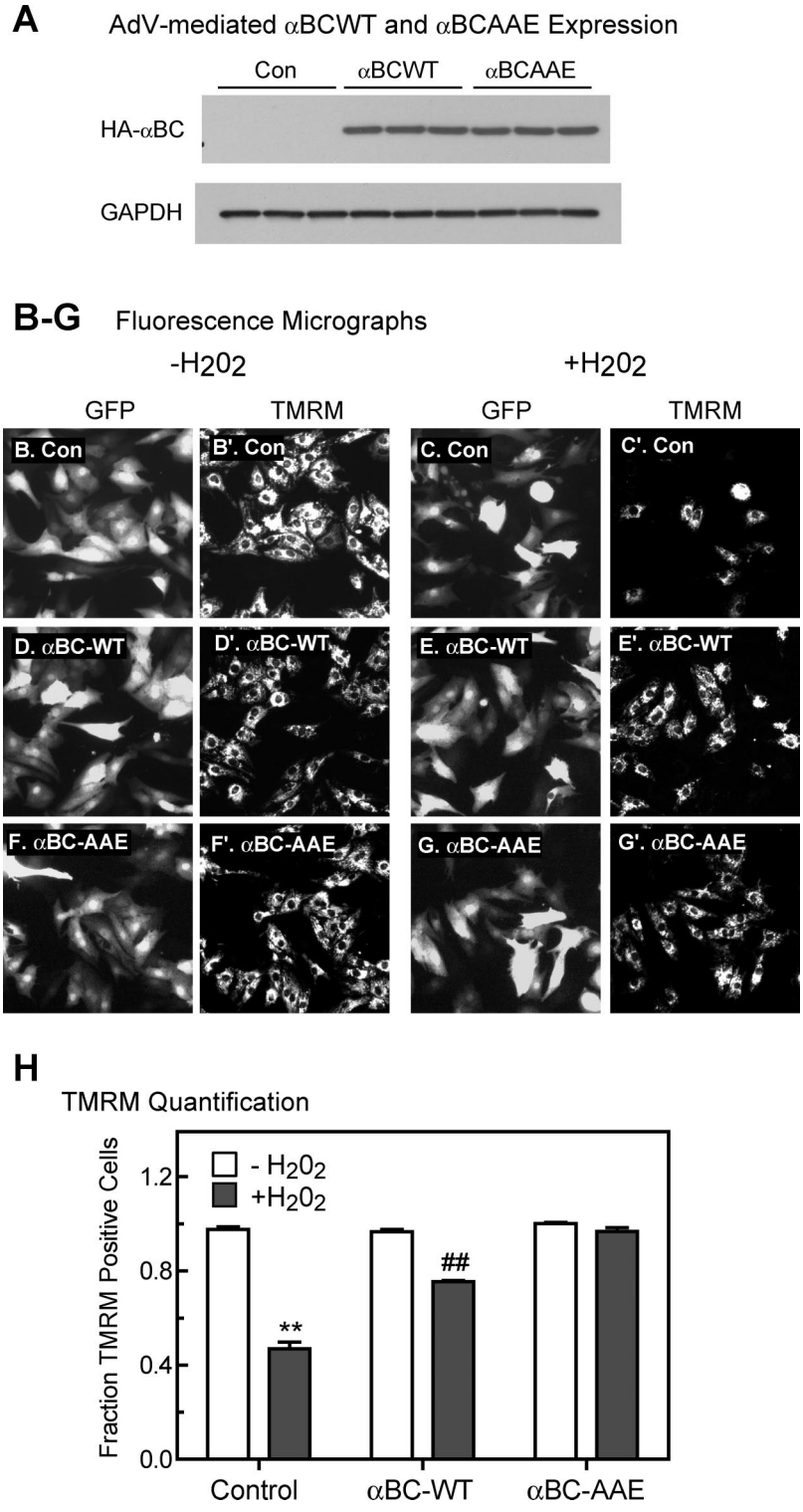

Fig. 7. Effect of αBC-WT or αBC-AAE on mitochondrial membrane potential in cultured cardiac myocytes. Cultured neonatal rat ventricular myocytes were infected with adenovirus (AdV) strains encoding no αBC (Con), hemagglutinin (HA)-tagged αBC-WT, or HA-αBC-AAE. All three AdV strains encode green fluorescence protein (GFP) driven off a cytomegalovirus promoter separate from that driving αBC expression. Cultures were treated with H_2O_2, incubated with tetramethylrhodamine methyl ester (TMRM), and viewed by fluorescence microscopy. *A*: immunoblots for HA and GAPDH demonstrated similar levels of HA-αBC-WT and HA-αBC-AAE expression. *B–G and B′–G′*: cultures were microscopically examined for GFP to demonstrate 100% transfection efficiency, as previously described, and to identify cells in each field (*B–G*). The same fields were then examined to identify TMRM fluorescence (*B′–G′*). *H*: each GFP-positive cell was scored for the presence of TMRM, and results are plotted as fraction of TMRM-positive GFP-positive cells (≥200 cells were counted per culture; $n = 3$ cultures per treatment). ** or ##$P < 0.01$ vs. all other treatments.

cells (23). In human lens epithelial cells, αBC binds to the proapoptotic, BH3-only proteins Bax and Bcl-x_S in the cytosol; this interaction inhibits translocation of these Bcl-2-binding proteins to mitochondria, which inhibits Bcl-2/Bax and Bcl-2/Bcl-x_S dimer formation, therefore moderating apoptosis (25).

In summary, the results of the present study demonstrate that αBC-S59P localizes to mitochondria of mouse hearts subjected to ex vivo I/R. Our previous findings that a mutant of αBC that mimics P-αBC-S59 (i.e., αBC-AAE) protects cultured cardiac myocytes from simulated I/R-mediated cell death (27) complements the present study, which showed that αBC-AAE inhibited calcium-induced MPT in vitro, and suggest further supporting cardioprotective roles for P-αBC-S59. It remains to be determined whether mitochondrial levels of other phosphorylated forms of αBC and/or nonphosphorylated αBC increase upon I/R stress. Thus it is possible that, in addition to P-αBC-

S59, these other forms of αBC also localize to mitochondria, where they could exert isoform-specific functions that are yet to be examined.

ACKNOWLEDGMENTS

We thank Donna Thuerauf and Marie Marcinko for expert technical assistance and review of the manuscript and Peter Belmont, Shirin Doroudgar, Mimi Ly, Archana Tadimalla, and John Vekitch for helpful discussions and review of the manuscript.

GRANTS

This work was supported by National Institutes of Health Grants HL-75573 and HL-085577. R. Whittaker is a Rees-Stealy Research Foundation/San Diego State University Heart Institute Fellow.

REFERENCES

1. **Armstrong SC.** Protein kinase activation and myocardial ischemia/reperfusion injury. *Cardiovasc Res* 61: 427–436, 2004.
2. **Bennardini F, Wrzosek A, Chiesi M.** αB-crystallin in cardiac tissue. Association with actin and desmin filaments. *Circ Res* 71: 288–294, 1992.
3. **Bhat SP, Nagineni CN.** αB subunit of lens-specific protein α-crystallin is present in other ocular and non-ocular tissues. *Biochem Biophys Res Commun* 158: 319–325, 1989.
4. **Bowers M, Ardehali H.** TOM20 and the heartbreakers: evidence for the role of mitochondrial transport proteins in cardioprotection. *J Mol Cell Cardiol* 41: 406–409, 2006.
5. **Bullard B, Ferguson C, Minajeva A, Leake MC, Gautel M, Labeit D, Ding L, Labeit S, Horwitz J, Leonard KR, Linke WA.** Association of the chaperone αB-crystallin with titin in heart muscle. *J Biol Chem* 279: 7917–7924, 2004.
6. **Chiesi M, Longoni S, Limbruno U.** Cardiac α-crystallin. III. Involvement during heart ischemia. *Mol Cell Biochem* 97: 129–136, 1990.
7. **Downs CA, Jones LR, Heckathorn SA.** Evidence for a novel set of small heat-shock proteins that associates with the mitochondria of murine PC12 cells and protects NADH:ubiquinone oxidoreductase from heat and oxidative stress. *Arch Biochem Biophys* 365: 344–350, 1999.
8. **Dubin RA, Wawrousek EF, Piatigorsky J.** Expression of the murine αB-crystallin gene is not restricted to the lens. *Mol Cell Biol* 9: 1083–1091, 1989.
9. **Ecroyd H, Meehan S, Horwitz J, Aquilina JA, Benesch JL, Robinson CV, Macphee CE, Carver JA.** Mimicking phosphorylation of αB-crystallin affects its chaperone activity. *Biochem J* 401: 129–141, 2007.
10. **Golenhofen N, Arbeiter A, Koob R, Drenckhahn D.** Ischemia-induced association of the stress protein αB-crystallin with I-band portion of cardiac titin. *J Mol Cell Cardiol* 34: 309–319, 2002.
11. **Golenhofen N, Ness W, Koob R, Htun P, Schaper W, Drenckhahn D.** Ischemia-induced phosphorylation and translocation of stress protein αB-crystallin to Z lines of myocardium. *Am J Physiol Heart Circ Physiol* 274: H1457–H1464, 1998.
12. **Halestrap AP, Clarke SJ, Javadov SA.** Mitochondrial permeability transition pore opening during myocardial reperfusion—a target for cardioprotection. *Cardiovasc Res* 61: 372–385, 2004.
13. **He L, Lemasters JJ.** Regulated and unregulated mitochondrial permeability transition pores: a new paradigm of pore structure and function? *FEBS Lett* 512: 1–7, 2002.
14. **Hoover HE, Thuerauf DJ, Martindale JJ, Glembotski CC.** αB-crystallin gene induction and phosphorylation by MKK6-activated p38. A potential role for αB-crystallin as a target of the p38 branch of the cardiac stress response. *J Biol Chem* 275: 23825–23833, 2000.
15. **Ito H, Kamei K, Iwamoto I, Inaguma Y, Garcia-Mata R, Sztul E, Kato K.** Inhibition of proteasomes induces accumulation, phosphorylation, and recruitment of HSP27 and αB-crystallin to aggresomes. *J Biochem (Tokyo)* 131: 593–603, 2002.
16. **Ito H, Okamoto K, Nakayama H, Isobe T, Kato K.** Phosphorylation of αB-crystallin in response to various types of stress. *J Biol Chem* 272: 29934–29941, 1997.
17. **Iwaki T, Kume-Iwaki A, Liem RK, Goldman JE.** αB-crystallin is expressed in non-lenticular tissues and accumulates in Alexander's disease brain. *Cell* 57: 71–78, 1989.
18. **Kadono T, Zhang XQ, Srinivasan S, Ishida H, Barry WH, Benjamin IJ.** CRYAB and HSPB2 deficiency increases myocyte mitochondrial permeability transition and mitochondrial calcium uptake. *J Mol Cell Cardiol* 40: 783–789, 2006.
19. **Kamradt MC, Chen F, Cryns VL.** The small heat shock protein αB-crystallin negatively regulates cytochrome *c*- and caspase-8-dependent activation of caspase-3 by inhibiting its autoproteolytic maturation. *J Biol Chem* 276: 16059–16063, 2001.
20. **Kamradt MC, Chen F, Sam S, Cryns VL.** The small heat shock protein αB-crystallin negatively regulates apoptosis during myogenic differentiation by inhibiting caspase-3 activation. *J Biol Chem* 277: 38731–38736, 2002.
21. **Kamradt MC, Lu M, Werner ME, Kwan T, Chen F, Strohecker A, Oshita S, Wilkinson JC, Yu C, Oliver PG, Duckett CS, Buchsbaum DJ, LoBuglio AF, Jordan VC, Cryns VL.** The small heat shock protein αB-crystallin is a novel inhibitor of TRAIL-induced apoptosis that suppresses the activation of caspase-3. *J Biol Chem* 280: 11059–11066, 2005.
22. **Lesnefsky EJ, Tandler B, Ye J, Slabe TJ, Turkaly J, Hoppel CL.** Myocardial ischemia decreases oxidative phosphorylation through cytochrome oxidase in subsarcolemmal mitochondria. *Am J Physiol Heart Circ Physiol* 273: H1544–H1554, 1997.
23. **Liu S, Li J, Tao Y, Xiao X.** Small heat shock protein αB-crystallin binds to p53 to sequester its translocation to mitochondria during hydrogen peroxide-induced apoptosis. *Biochem Biophys Res Commun* 354: 109–114, 2007.
24. **Longoni S, Lattonen S, Bullock G, Chiesi M.** Cardiac α-crystallin. II. Intracellular localization. *Mol Cell Biochem* 97: 121–128, 1990.
25. **Mao YW, Liu JP, Xiang H, Li DW.** Human αA- and αB-crystallins bind to Bax and Bcl-X_S to sequester their translocation during staurosporine-induced apoptosis. *Cell Death Differ* 11: 512–526, 2004.
26. **Martindale JJ, Wall JA, Martinez-Longoria DM, Aryal P, Rockman HA, Guo Y, Bolli R, Glembotski CC.** Overexpression of mitogen-activated protein kinase kinase 6 in the heart improves functional recovery from ischemia in vitro and protects against myocardial infarction in vivo. *J Biol Chem* 280: 669–676, 2005.
27. **Morrison LE, Hoover HE, Thuerauf DJ, Glembotski CC.** Mimicking phosphorylation of αB-crystallin on serine-59 is necessary and sufficient to provide maximal protection of cardiac myocytes from apoptosis. *Circ Res* 92: 203–211, 2003.
28. **Morrison LE, Whittaker RJ, Klepper RE, Wawrousek EF, Glembotski CC.** Roles for αB-crystallin and HSPB2 in protecting the myocardium from ischemia-reperfusion-induced damage in a KO mouse model. *Am J Physiol Heart Circ Physiol* 286: H847–H855, 2004.
29. **Palmer JW, Tandler B, Hoppel CL.** Biochemical properties of subsarcolemmal and interfibrillar mitochondria isolated from rat cardiac muscle. *J Biol Chem* 252: 8731–8739, 1977.
30. **Rane MJ, Coxon PY, Powell DW, Webster R, Klein JB, Pierce W, Ping P, McLeish KR.** p38 Kinase-dependent MAPKAPK-2 activation functions as 3-phosphoinositide-dependent kinase-2 for Akt in human neutrophils. *J Biol Chem* 276: 3517–3523, 2001.
31. **Ray PS, Martin JL, Swanson EA, Otani H, Dillmann WH, Das DK.** Transgene overexpression of αB crystallin confers simultaneous protection against cardiomyocyte apoptosis and necrosis during myocardial ischemia and reperfusion. *FASEB J* 15: 393–402, 2001.
32. **Singh BN, Rao KS, Ramakrishna T, Rangaraj N, Rao CM.** Association of αB-crystallin, a small heat shock protein, with actin: role in modulating actin filament dynamics in vivo. *J Mol Biol* 366: 756–767, 2007.
33. **Taylor RP, Benjamin IJ.** Small heat shock proteins: a new classification scheme in mammals. *J Mol Cell Cardiol* 38: 433–444, 2005.
34. **Thuerauf DJ, Marcinko M, Gude N, Rubio M, Sussman MA, Glembotski CC.** Activation of the unfolded protein response in infarcted mouse heart and hypoxic cultured cardiac myocytes. *Circ Res* 99: 275–282, 2006.
35. **Wall JA, Wei J, Ly M, Belmont P, Martindale JJ, Tran D, Sun J, Chen WJ, Yu W, Oeller P, Briggs S, Gustafsson AB, Sayen MR, Gottlieb RA, Glembotski CC.** Alterations in oxidative phosphorylation complex proteins in the hearts of transgenic mice that overexpress the p38 MAP kinase activator, MAP kinase kinase 6. *Am J Physiol Heart Circ Physiol* 291: H2462–H2472, 2006.
36. **Yaung J, Jin M, Barron E, Spee C, Wawrousek EF, Kannan R, Hinton DR.** α-Crystallin distribution in retinal pigment epithelium and effect of gene knockouts on sensitivity to oxidative stress. *Mol Vis* 13: 566–577, 2007.
37. **Zheng C, Lin Z, Zhao ZJ, Yang Y, Niu H, Shen X.** MAPK-activated protein kinase-2 (MK2)-mediated formation and phosphorylation-regulated dissociation of the signal complex consisting of p38, MK2, Akt, and Hsp27. *J Biol Chem* 281: 37215–37226, 2006.